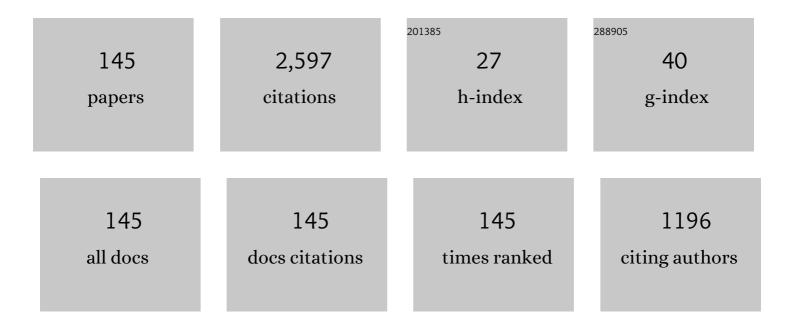
List of Publications by Year in descending order

Source: https://exaly.com/author-pdf/5253312/publications.pdf Version: 2024-02-01



YAN-OINC SU

#	Article	IF	CITATIONS
1	Microstructure and mechanical properties of Ti44Al6Nb1Cr2V alloy after gaseous hydrogen charging at 1373–1693ÂK. Rare Metals, 2023, 42, 664-671.	3.6	1
2	Manipulating internal flow units toward favorable plasticity in Zr-based bulk-metallic glasses by hydrogenation. Journal of Materials Science and Technology, 2022, 102, 36-45.	5.6	16
3	Significant enhancement of the corrosion performance of Ti-6Al-3Nb-2Zr-1Mo alloy via carbon addition in reducing acid environment. Materials Letters, 2022, 306, 130939.	1.3	6
4	Microstructure and mechanical properties of multi-phase reinforced Hf-Mo-Nb-Ti-Zr refractory high-entropy alloys. International Journal of Refractory Metals and Hard Materials, 2022, 102, 105723.	1.7	20
5	Effect of processing parameters on the microstructure and mechanical properties of TiAl/Ti2AlNb laminated composites. Journal of Materials Science and Technology, 2022, 109, 228-244.	5.6	19
6	On the solidification behaviors of AlCu5MnCdVA alloy in electron beam freeform fabrication: Microstructural evolution, Cu segregation and cracking resistance. Additive Manufacturing, 2022, 51, 102606.	1.7	3
7	Effect of growth rate on microstructure evolution in directionally solidified Ti–47Al alloy. Heliyon, 2022, 8, e08704.	1.4	1
8	Corrosion behaviour of a wrought Ti-6Al-3Nb-2Zr-1Mo alloy in artificial seawater with various fluoride concentrations and pH values. Materials and Design, 2022, 214, 110416.	3.3	17
9	Enhanced strength and fracture characteristics of the TiAl/Ti2AlNb laminated composite. Materials Science & Engineering A: Structural Materials: Properties, Microstructure and Processing, 2022, 835, 142632.	2.6	8
10	In-situ study on γ phase transformation behaviour of γ-TiAl alloys at different cooling rates. Progress in Natural Science: Materials International, 2022, 32, 345-357.	1.8	9
11	Tuning microstructure and improving the corrosion resistance of Ti-6Al-3Nb-2Zr-1Mo alloy using the electron beam freeform fabrication. Chemical Engineering Journal, 2022, 444, 136524.	6.6	9
12	Tailoring formation and proportion of strengthening phase in non-equiatomic CoCrFeNi high entropy alloy by alloying Si element. Intermetallics, 2022, 147, 107617.	1.8	9
13	Solidification behavior and microstructure evolution of Nb-Si-Mo alloy in ultrasonic field. International Journal of Refractory Metals and Hard Materials, 2022, 108, 105933.	1.7	5
14	Optimizing the microstructures and mechanical properties of Al-Cu-based alloys with large solidification intervals by coupling travelling magnetic fields with sequential solidification. Journal of Materials Science and Technology, 2021, 61, 100-113.	5.6	18
15	Annealed microstructure dependent corrosion behavior of Ti-6Al-3Nb-2Zr-1Mo alloy. Journal of Materials Science and Technology, 2021, 62, 234-248.	5.6	68
16	In-situ investigation of β/α transformation in β-solidifying γ-TiAl alloys at different cooling rates. Materials Letters, 2021, 285, 129092.	1.3	6
17	The corrosion behavior of Ti-6Al-3Nb-2Zr-1Mo alloy: Effects of HCl concentration and temperature. Journal of Materials Science and Technology, 2021, 74, 143-154.	5.6	43
18	Optimizing microstructure, shrinkage defects and mechanical performance of ZL205A alloys via coupling travelling magnetic fields with unidirectional solidification. Journal of Materials Science and Technology, 2021, 74, 246-258.	5.6	16

#	Article	IF	CITATIONS
19	Eliminating shrinkage defects and improving mechanical performance of large thin-walled ZL205A alloy castings by coupling travelling magnetic fields with sequential solidification. Transactions of Nonferrous Metals Society of China, 2021, 31, 865-877.	1.7	7
20	Impact of laser scanning speed on microstructure and mechanical properties of Inconel 718 alloys by selective laser melting. China Foundry, 2021, 18, 170-179.	0.5	8
21	Influence of laser parameters on segregation of Nb during selective laser melting of Inconel 718. China Foundry, 2021, 18, 379-388.	0.5	3
22	The interface structure and its impact on the mechanical behavior of TiAl/Ti2AlNb laminated composites. Materials Science & Engineering A: Structural Materials: Properties, Microstructure and Processing, 2021, 827, 142095.	2.6	14
23	Design a novel TiAl/Ti2AlNb laminated composite with high toughness prepared by foil-foil metallurgy. Materials Letters, 2021, 303, 130463.	1.3	8
24	Effect of zirconium content on the microstructure and corrosion behavior of as-cast Ti-Al-Nb-Zr-Mo alloy. Journal of Materials Research and Technology, 2021, 15, 4896-4913.	2.6	31
25	Microstructure evolution, Cu segregation and tensile properties of CoCrFeNiCu high entropy alloy during directional solidification. Journal of Materials Science and Technology, 2020, 38, 19-27.	5.6	85
26	An as-cast high-entropy alloy with remarkable mechanical properties strengthened by nanometer precipitates. Nanoscale, 2020, 12, 3965-3976.	2.8	49
27	A Comparative Study on Microstructure and Mechanical Properties of Tiâ€43/46Al–5Nb–0.1B Alloys Modified by Mo. Advanced Engineering Materials, 2020, 22, 1901075.	1.6	6
28	In-situ observation microstructure evolution and growth kinetics of lamellar γ phases in Ti44Al alloy during heat treatment. Journal of Materials Research and Technology, 2020, 9, 12157-12166.	2.6	5
29	Microstructures and mechanical properties of Ti–44Al–5Nb–3Cr–1.5Zr–xMo–yB alloys. Journal of Materials Research, 2020, 35, 2756-2764.	1.2	4
30	Thermal deformation behavior of γ-TiAl based alloy by plasma hydrogenation. International Journal of Hydrogen Energy, 2020, 45, 34214-34226.	3.8	6
31	Microstructural evolution of Al-Cu-Li alloys with different Li contents by coupling of near-rapid solidification and two-stage homogenization treatment. China Foundry, 2020, 17, 190-197.	0.5	10
32	Effect of melt hydrogenation on microstructure evolution and tensile properties of (TiB + TiC)/Ti-6Al-4V composites. Journal of Materials Research and Technology, 2020, 9, 6343-6351.	2.6	10
33	Effect of hydrogen on interfacial reaction between Ti-6Al-4V alloy melt and graphite mold. Journal of Materials Research and Technology, 2020, 9, 6933-6939.	2.6	5
34	Microstructure and mechanical properties of CoCrFeNiW high entropy alloys reinforced by μ phase particles. Journal of Alloys and Compounds, 2020, 843, 155997.	2.8	49
35	The growth behavior of columnar grains in a TiAl alloy during directional induction heat treatments. CrystEngComm, 2020, 22, 1188-1196.	1.3	8
36	Impact of hydrogen microalloying on the mechanical behavior of Zr-bearing metallic glasses: A molecular dynamics study. Journal of Materials Science and Technology, 2020, 45, 198-206.	5.6	16

#	Article	IF	CITATIONS
37	Study on dispersion of Ti2AlC particle and formation of columnar crystal with different solidification rates during CCDS TiAl-based composite. Journal of Alloys and Compounds, 2020, 832, 154893.	2.8	5
38	Microstructure and microhardness of Ti-48Al alloy prepared by rapid solidification. China Foundry, 2020, 17, 429-434.	0.5	5
39	Microstructures and phase transformation in directionally solidified TiAl-Nb alloys. China Foundry, 2020, 17, 402-408.	0.5	Ο
40	Microstructure and mechanical properties of NbZrTi and NbHfZrTi alloys. Rare Metals, 2019, 38, 840-847.	3.6	22
41	Improving microstructure and mechanical properties of Ti43Al5Nb0.1B alloy by addition of Fe. Rare Metals, 2019, 38, 1024-1032.	3.6	11
42	Microstructure, tensile properties and creep behavior of high-Al TiAlNb alloy using electromagnetic cold crucible continuous casting. Journal of Alloys and Compounds, 2019, 801, 166-174.	2.8	11
43	A novel method to prepare columnar grains of TiAl alloys by controlling induction heating. International Communications in Heat and Mass Transfer, 2019, 108, 104315.	2.9	17
44	Formation of Ti2AlN and TiB and its effect on mechanical properties of Ti46Al4Nb1Mo alloy by adding BN particles. Materials Science & Engineering A: Structural Materials: Properties, Microstructure and Processing, 2019, 756, 161-171.	2.6	16
45	Investigation of shear transformation zone and ductility of Zr-based bulk metallic glass after plasma-assisted hydrogenation. Materials Science & Engineering A: Structural Materials: Properties, Microstructure and Processing, 2019, 759, 105-111.	2.6	21
46	Hot-deformation behaviour and hot-processing map of melt-hydrogenated Ti 6Al 4V/(TiB+TiC). International Journal of Hydrogen Energy, 2019, 44, 8641-8649.	3.8	18
47	Boride Formation, Microstructure Evolution, and Mechanical Properties of Ti42Al6Nb2.6C0.8Ta Alloyed by Boron. Advanced Engineering Materials, 2019, 21, 1800934.	1.6	3
48	Microstructure and Mechanical Properties of Bioâ€Inspired Ti/Al/Alâ€C <sub>f</sub> Multilayered Composites. Advanced Engineering Materials, 2019, 21, 1800722.	1.6	2
49	Microstructures and properties of Nbâ $\in$ "Si-based alloys with B addition. Rare Metals, 2019, , 1.	3.6	Ο
50	High-throughput analysis of Al and Nb effects on mechanical behaviour of TiAl alloys using electromagnetic cold crucible continuous casting. Journal of Alloys and Compounds, 2019, 775, 124-131.	2.8	9
51	Strengthening FCC-CoCrFeMnNi high entropy alloys by Mo addition. Journal of Materials Science and Technology, 2019, 35, 578-583.	5.6	126
52	Effects of V and B, Y additions on the microstructure and creep behaviour of high-Nb TiAl alloys. Journal of Alloys and Compounds, 2018, 747, 640-647.	2.8	33
53	Macro/microstructure evolution and mechanical properties of Ti33.3Al alloys by adding WC particles. Materials Science & Engineering A: Structural Materials: Properties, Microstructure and Processing, 2018, 725, 171-180.	2.6	8
54	Effects of hydrogen on the interfacial reaction between Ti 6Al 4V alloy melt and Al2O3 ceramic shell. International Journal of Hydrogen Energy, 2018, 43, 5225-5230.	3.8	3

#	Article	IF	CITATIONS
55	Creep Behavior of Highâ€Nb TiAl Alloy at 800–900 °C by Directional Solidification. Advanced Engineering Materials, 2018, 20, 1700734.	1.6	6
56	Microstructure control and creep behavior of Ti-47Al-6Nb-0.1C alloy by directional solidification. Intermetallics, 2018, 94, 152-159.	1.8	23
57	Hydrogen induced microstructure evolution of titanium matrix composites. International Journal of Hydrogen Energy, 2018, 43, 9838-9847.	3.8	16
58	Brittle–ductile transition during creep in nearly and fully lamellar high-Nb TiAl alloys. Intermetallics, 2018, 93, 47-54.	1.8	38
59	Positive effect of hydrogen on interface of in situ synthesized Ti-6Al-4V matrix composites. Materials Science & Engineering A: Structural Materials: Properties, Microstructure and Processing, 2018, 711, 12-21.	2.6	8
60	Effect of Zr on microstructure and mechanical properties of binary TiAl alloys. Transactions of Nonferrous Metals Society of China, 2018, 28, 1724-1734.	1.7	9
61	Microstructure and mechanical properties of Ti43Al6Nb alloys with different zirconium contents. Rare Metals, 2018, , 1.	3.6	3
62	Microstructure evolution and mechanical properties of TiAl binary alloys added with SiC fibers. Intermetallics, 2018, 98, 69-78.	1.8	26
63	Microstructure, Mechanical Properties, and Crack Propagation Behavior in High-Nb TiAl Alloys by Directional Solidification. Metallurgical and Materials Transactions A: Physical Metallurgy and Materials Science, 2018, 49, 4555-4564.	1.1	39
64	Effect of a Traveling Magnetic Field on Micropore Formation in Al-Cu Alloys. Metals, 2018, 8, 448.	1.0	4
65	Effects of grain size and precipitated phases on mechanical properties in TiAl gradient materials. Materials Science & Engineering A: Structural Materials: Properties, Microstructure and Processing, 2018, 731, 634-641.	2.6	11
66	Optimization of electromagnetic energy in cold crucible used for directional solidification of TiAl alloy. Energy, 2018, 161, 143-155.	4.5	13
67	Effect of β-phase stabilizing elements and high temperature (1373–1693ÂK) on hydrogen absorption in TiAl alloys. International Journal of Hydrogen Energy, 2017, 42, 86-95.	3.8	17
68	Influence of high-temperature hydrogen charging on microstructure and hot deformability of binary TiAl alloys. Journal of Alloys and Compounds, 2017, 701, 399-407.	2.8	9
69	Hydrogen induced softening and hardening for hot workability of (TiBÂ+ÂTiC)/Ti-6Al-4V composites. International Journal of Hydrogen Energy, 2017, 42, 3380-3388.	3.8	16
70	High temperature deformation behavior of melt hydrogenated (TiB + TiC)/Ti-6Al-4V composites. Materials and Design, 2017, 121, 335-344.	3.3	33
71	A novel method to directional solidification of TiAlNb alloys by mixing binary TiAl ingot and Nb wire. Materials Science & Engineering A: Structural Materials: Properties, Microstructure and Processing, 2017, 687, 181-192.	2.6	16
72	Continuous Casting of TiAlNb Alloys with Different Velocities by Mixing Binary TiAl Ingot and Nb Wire. Advanced Engineering Materials, 2017, 19, 1700058.	1.6	0

#	Article	IF	CITATIONS
73	Characterization of p-type multicrystalline silicon prepared by cold crucible continuous melting and directional solidification. Materials Science in Semiconductor Processing, 2017, 68, 62-67.	1.9	4
74	Microstructure modification and mechanical performances enhancement of Ti44Al6Nb1Cr alloy by ultrasound treatment. Journal of Alloys and Compounds, 2017, 710, 409-417.	2.8	25
75	Hydrogen-induced softening of Ti–44Al–6Nb–1Cr–2V alloy during hot deformation. International Journal of Hydrogen Energy, 2017, 42, 8329-8337.	3.8	19
76	Effects of hydrogen on the nanomechanical properties of a bulk metallic glass during nanoindentation. International Journal of Hydrogen Energy, 2017, 42, 25436-25445.	3.8	14
77	Microstructures and mechanical properties of melt hydrogenated Nb-Si based alloy. International Journal of Hydrogen Energy, 2017, 42, 26417-26422.	3.8	4
78	Numerical Research on Magnetic Field, Temperature Field and Flow Field During Melting and Directionally Solidifying TiAl Alloys by Electromagnetic Cold Crucible. Metallurgical and Materials Transactions B: Process Metallurgy and Materials Processing Science, 2017, 48, 3345-3358.	1.0	11
79	Hot deformation behavior and dynamic recrystallization of melt hydrogenated Ti-6Al-4V alloy. Journal of Alloys and Compounds, 2017, 728, 709-718.	2.8	32
80	Removal of metal impurities in metallurgical grade silicon by cold crucible continuous melting and directional solidification. Separation and Purification Technology, 2017, 188, 67-72.	3.9	23
81	Hydrogen-induced amorphization of Zr-Cu-Ni-Al alloy. China Foundry, 2017, 14, 145-150.	0.5	0
82	Experimental and numerical investigation on mass transfer induced by electromagnetic field in cold crucible used for directional solidification. International Journal of Heat and Mass Transfer, 2017, 114, 297-306.	2.5	29
83	Effect of hydrogen addition on the mechanical properties of a bulk metallic glass. Journal of Alloys and Compounds, 2017, 695, 3183-3190.	2.8	19
84	Mass transfer behaviors of oxygen during cold crucible continuous casting silicon. International Journal of Heat and Mass Transfer, 2016, 100, 428-432.	2.5	9
85	Microstructures, micro-segregation and solidification path of directionally solidified Ti-45Al-5Nb alloy. China Foundry, 2016, 13, 107-113.	0.5	11
86	The hydrogen absorption behavior of high Nb contained titanium aluminides under high pressure and temperature. International Journal of Hydrogen Energy, 2016, 41, 13254-13260.	3.8	13
87	Deformation behavior and microstructural evolution of hydrogenated Ti44Al6Nb alloy during thermo-compression at 1373–1523 K. Materials and Design, 2016, 108, 259-268.	3.3	28
88	Effect of growth rate on microstructures and microhardness in directionally solidified Ti–47Al–1.0W–0.5Si alloy. Journal of Materials Research, 2016, 31, 618-626.	1.2	3
89	Lamellar orientation control of Ti–47Al–0.5W–0.5Si by directional solidification using β seeding technique. Intermetallics, 2016, 73, 1-4.	1.8	8
90	Influence of thermal stabilization treatment on microstructure evolution of the mushy zone and subsequent directional solidification in Ti-43Al-3Si alloy. Materials and Design, 2016, 97, 392-399.	3.3	14

#	Article	IF	CITATIONS
91	Investigation of macro/microstructure evolution and mechanical properties of directionally solidified high-Nb TiAl-based alloy. Materials and Design, 2016, 89, 492-506.	3.3	53
92	Effect of heat treatment on microstructure and mechanical properties of cast and directionally solidified high-Nb contained TiAl-based alloys. Journal of Materials Research, 2015, 30, 3331-3342.	1.2	5
93	Continued growth controlling of the non-preferred primary phase for the parallel lamellar structure in directionally solidified Ti–50Al–4Nb alloy. Journal of Alloys and Compounds, 2015, 632, 152-160.	2.8	14
94	Microstructure and room temperature tensile property of as-cast Ti44Al6Nb1.0Cr2.0V alloy. Transactions of Nonferrous Metals Society of China, 2015, 25, 1097-1105.	1.7	6
95	Deformation behavior and microstructural evolution of directionally solidified TiAlNb-based alloy during thermo-compression at 1373–1573K. Materials and Design, 2015, 84, 118-132.	3.3	57
96	Effect of solidification parameters on microstructural characteristics and mechanical properties of directionally solidified binary TiAl alloy. Journal of Alloys and Compounds, 2015, 650, 8-14.	2.8	20
97	Effect of cyclic heat treatment on microstructures and mechanical properties of directionally solidified Ti–46Al–6Nb alloy. Transactions of Nonferrous Metals Society of China, 2015, 25, 1872-1880.	1.7	13
98	Effect of power on microstructure and mechanical properties of Ti44Al6Nb1.0Cr2.0V0.15Y0.1B alloy prepared by cold crucible directional solidification. Materials & Design, 2015, 67, 390-397.	5.1	27
99	Microstructure evolution and mechanical properties of directionally-solidified TiAlNb alloy in different temperature gradients. Journal of Alloys and Compounds, 2015, 648, 667-675.	2.8	33
100	Effect of growth rate and diameter on microstructure and hardness of directionally solidified Ti–46Al–8Nb alloy. Transactions of Nonferrous Metals Society of China, 2014, 24, 4044-4052.	1.7	6
101	Faceted–nonfaceted growth transition and 3-D morphological evolution of primary Al <sub>6</sub> Mn microcrystals in directionally solidified Al–3 at.% Mn alloy. Journal of Materials Research, 2014, 29, 1256-1263.	1.2	18
102	The influence of melt hydrogenation on Ti600 alloy. International Journal of Hydrogen Energy, 2014, 39, 6089-6094.	3.8	9
103	Electrical resistivity distribution of silicon ingot grown by cold crucible continuous melting and directional solidification. Materials Science in Semiconductor Processing, 2014, 23, 14-19.	1.9	7
104	Microstructure control and mechanical properties of Ti44Al6Nb1.0Cr2.0V alloy by cold crucible directional solidification. Materials Science & Engineering A: Structural Materials: Properties, Microstructure and Processing, 2014, 614, 67-74.	2.6	40
105	Local melting/solidification during peritectic solidification in a steep temperature gradient: analysis of a directionally solidified Al–25at%Ni. Applied Physics A: Materials Science and Processing, 2014, 116, 1821-1831.	1.1	9
106	Influence of initial solid–liquid interface morphology on further microstructure evolution during directional solidification. Applied Physics A: Materials Science and Processing, 2013, 110, 443-451.	1.1	6
107	Characterization of microstructural length scales in directionally solidified Sn–36%Ni peritectic alloy. Transactions of Nonferrous Metals Society of China, 2013, 23, 2446-2453.	1.7	2
108	Uniformity analysis of magnetic field in an electromagnetic cold crucible used for directional solidification. COMPEL - the International Journal for Computation and Mathematics in Electrical and Electronic Engineering, 2013, 32, 997-1008.	0.5	4

#	Article	IF	CITATIONS
109	Flow field and its effect on microstructure in cold crucible directional solidification of Nb containing TiAl alloy. Journal of Materials Processing Technology, 2013, 213, 1355-1363.	3.1	21
110	A lateral remelting phenomenon of the primary phase below the temperature of peritectic reaction in directionally solidified Cu–Ge alloys. Journal of Materials Research, 2013, 28, 3261-3269.	1.2	11
111	Two-phase separated growth and peritectic reaction during directional solidification of Cu–Ge peritectic alloys. Journal of Materials Research, 2013, 28, 1372-1377.	1.2	5
112	Characterization of hydrogen-induced structural changes in Zr-based bulk metallic glasses using positron annihilation spectroscopy. Journal of Materials Research, 2012, 27, 2587-2592.	1.2	4
113	Fabrication of wavy $\hat{I}^3$ -TiAl based sheet with foil metallurgy. Transactions of Nonferrous Metals Society of China, 2012, 22, 72-77.	1.7	7
114	Temperature field calculation on cold crucible continuous melting and directional solidifying Ti50Al alloys. Transactions of Nonferrous Metals Society of China, 2012, 22, 647-653.	1.7	9
115	Microstructure, microsegregation pattern and the formation of B2 phase in directionally solidified Ti–46Al–8Nb alloy. Journal of Alloys and Compounds, 2012, 541, 275-282.	2.8	34
116	Lamellar orientation and growth direction of ${\rm \hat{l}}\pm$ phase in directionally solidified Ti-46Al-0.5W-0.5Si alloy. Intermetallics, 2012, 27, 38-45.	1.8	25
117	Morphological characteristics of triple junction region and process of the peritectic reaction during directional solidification of Cu–Ge alloys. Journal of Alloys and Compounds, 2012, 539, 44-49.	2.8	8
118	Microstructure and microsegregation in directionally solidified Ti–46Al–8Nb alloy. Transactions of Nonferrous Metals Society of China, 2012, 22, 1342-1349.	1.7	11
119	Enhanced plasticity in Zr-based bulk metallic glasses by hydrogen. International Journal of Hydrogen Energy, 2012, 37, 14697-14701.	3.8	42
120	Bulk metallic glass formation: The positive effect of hydrogen. Journal of Non-Crystalline Solids, 2012, 358, 2606-2611.	1.5	17
121	Secondary dendrite arm migration caused by temperature gradient zone melting during peritectic solidification. Acta Materialia, 2012, 60, 2679-2688.	3.8	41
122	Effect of growth rate on microstructure parameters and microhardness in directionally solidified Ti–49Al alloy. Materials & Design, 2012, 34, 552-558.	5.1	39
123	Deoxidation of bulk metallic glasses by hydrogen arc melting. Materials Letters, 2012, 83, 1-3.	1.3	12
124	First Phase Selection in Solid Ti/Al Diffusion Couple. Rare Metal Materials and Engineering, 2011, 40, 753-756.	0.8	21
125	Effect of parameters on the grain growth of silicon ingots prepared by electromagnetic cold crucible continuous casting. Journal of Crystal Growth, 2011, 332, 68-74.	0.7	11
126	Microstructure evolution in directionally solidified Ti–(50, 52)at%Al alloys. Intermetallics, 2011, 19, 175-181.	1.8	20

#	Article	IF	CITATIONS
127	Effect of traveling magnetic field on gas porosity during solidification. Transactions of Nonferrous Metals Society of China, 2011, 21, 1981-1985.	1.7	4
128	Dependency of microstructure parameters and microhardness on the temperature gradient for directionally solidified Ti–49Al alloy. Materials Chemistry and Physics, 2011, 130, 1232-1238.	2.0	27
129	Directional solidification of Ti–49 at.%Al alloy. Applied Physics A: Materials Science and Processing, 2011, 105, 239-248.	1.1	16
130	Investigation of melt hydrogenation on the microstructure and deformation behavior of Ti–6Al–4V alloy. International Journal of Hydrogen Energy, 2011, 36, 1027-1036.	3.8	29
131	Influence of thermal stabilization on the solute concentration of the melt in directional solidification. Journal of Crystal Growth, 2010, 312, 3658-3664.	0.7	25
132	Hydrogen solubility in molten TiAl alloys. International Journal of Hydrogen Energy, 2010, 35, 8008-8013.	3.8	23
133	Deoxidation of Ti–Al intermetallics via hydrogen treatment. International Journal of Hydrogen Energy, 2010, 35, 9214-9217.	3.8	17
134	Effect of hydrogen on hot deformation behaviors of TiAl alloys. International Journal of Hydrogen Energy, 2010, 35, 13322-13328.	3.8	35
135	EFFECT OF <font>HfO</font> <sub>2</sub> -CODOPING CONCENTRATION ON THE OPTICAL PROPERTIES OF <font>Er</font> <sup>3+</sup> -DOPED <font>LiNbO</font> <sub>3</sub> . Modern Physics Letters B, 2010, 24, 495-502.	1.0	3
136	Dependency of microhardness on solidification processing parameters and microstructure characteristics in the directionally solidified Ti–46Al–0.5W–0.5Si alloy. Journal of Alloys and Compounds, 2010, 504, 60-64.	2.8	49
137	The microstructure parameters and microhardness of directionally solidified Ti–43Al–3Si alloy. Journal of Alloys and Compounds, 2010, 506, 593-599.	2.8	50
138	Effect of electromagnetic force on melt induced by traveling magnetic field. Transactions of Nonferrous Metals Society of China, 2010, 20, 662-667.	1.7	10
139	EFFECT OF <font>Li/Nb</font> RATIO ON GROWTH AND SPECTROMETRIC CHARACTERIZATION OF <font>Hf</font> : <font>E</font> LiNbO <sub>3</sub> CRYSTALS. Modern Physics Letters B, 2009, 23, 1557-1565.	1.0	3
140	JUDD–OFELT THEORY ANALYSIS AND SPECTROSCOPIC PROPERTIES OF Ho:LiNbO3. Modern Physics Letters B, 2009, 23, 3235-3242.	1.0	1
141	Deoxidation of Titanium alloy using hydrogen. International Journal of Hydrogen Energy, 2009, 34, 8958-8963.	3.8	53
142	Effects of hydrogenation on ambient deformation behaviors of Ti-45Al alloy. Transactions of Nonferrous Metals Society of China, 2009, 19, s403-s408.	1.7	4
143	Formation of titanium hydride in Ti–6Al–4V alloy. Journal of Alloys and Compounds, 2006, 425, 140-144.	2.8	63
144	Microstructure selection during the directionally peritectic solidification of Ti–Al binary system. Intermetallics, 2005, 13, 267-274.	1.8	56

#	Article	IF	CITATIONS
145	Effects of Heating Power on Microstructure Evolution and Tensile Properties at Elevated Temperature by Directional Solidification for Ti2AlC/TiAl Composites. Advanced Engineering Materials, 0, , 2100736.	1.6	1